

Supporting Information

Before comparing the scaling parameter developed by Bartlett *et al.* [1] with our proposed scaling parameter, it would be beneficial to go over the assumptions that are made leading to $\sqrt{A'/C}$ scaling parameter. First, it is assumed that the system is in equilibrium such that $\partial\Pi/\partial A' = 0$, where Π is the total energy of the system and A' is bond area. Second, it is assumed that upon reaching a critical force the interface will separate in an unstable manner in a single step such that $\partial^2\Pi/\partial A'^2 < 0$. Finally, the system is assumed to conserve energy leading to a catastrophic failure where any change is larger than the system size. Owing to the third assumption, the derivative of system energy is reduced to the algebraic expression leading to $\sqrt{A'/C}$ instead of $\sqrt{\partial A'/\partial C}$.

Now that we have a closed-form solution for the system compliance, we can compare two scaling parameters (assuming constant crack propagation velocity) to show in what conditions these two scaling relationships deviate from each other. Here are the expressions for the two scaling parameters:

$$\frac{A'}{C} = \frac{wL_B}{\frac{h_A\lambda}{wG}\text{Coth}(\lambda L_B) + \frac{L_F}{E h_B w} + C_M} \quad (1)$$

$$\frac{\partial A'}{\partial C} = \frac{E h_B w^2 \text{Sinh}^2(\lambda L_B)}{1 + \text{Sinh}^2(\lambda L_B)} \quad (2)$$

First, we can find that $\sqrt{A'/C}$ is a function of free length (L_F) and machine compliance (C_M) whereas $\sqrt{\partial A'/\partial C}$ is not. As seen in Figure 1, $\sqrt{A'/C}$ decreases as the ratio of free length over shear lag characteristic length (L_F/L_{lag}) increases, which is due to the added compliance from the free length. On the other hand, $\sqrt{\partial A'/\partial C}$ does not change as the free length or machine compliance increases. Therefore, we would expect a higher slope of maximum shear force capacity versus $\sqrt{A'/C}$ for the samples with higher load train compliance (longer free length or softer testing machine), while the slope is not expected to change when the force capacity is plotted as a function of $\sqrt{\partial A'/\partial C}$. Moreover, Figure 1 depicts the change in $\sqrt{A'/C}$ and $\sqrt{\partial A'/\partial C}$ as a function of the ratio of bond length over shear lag characteristic length (L_B/L_{lag}) while the L_F and C_M are kept constant. It is clear that around the bond length twice the characteristic length, we see a deviation between $\sqrt{A'/C}$ and $\sqrt{\partial A'/\partial C}$ approaches. Interestingly, it is close to the length scale in which the transition from catastrophic to progressive failures occurs. Overall, there are two conditions at which we would expect the two models deviate from each other: (I) By increasing the load train compliance (by increasing the free length or machine compliance), (II) by transition from catastrophic failure to progressive failure.

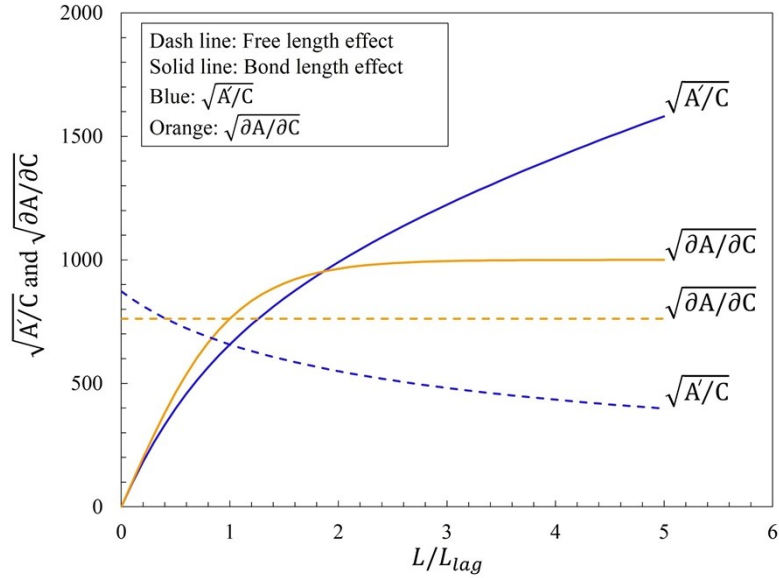


Figure 1. Changes in $\sqrt{A/C}$ and $\sqrt{\partial A/\partial C}$ as a function of normalized length. Dash line refers to free length effect. The solid line corresponds to the bond length effect. Blue and orange colors refer to $\sqrt{A/C}$ and $\sqrt{\partial A/\partial C}$, respectively.

Figure 2 exhibits the force versus displacement curves for the PSA tapes with the same bond area, but different free lengths. The total system compliance increases significantly by increasing the free length, while there is a slight change in the maximum force of the PSA tapes. The change in the maximum force is due to the viscoelastic response of the PSA, as by changing the free length the displacement rate changes, giving rise to the rate dependent response of the PSA.

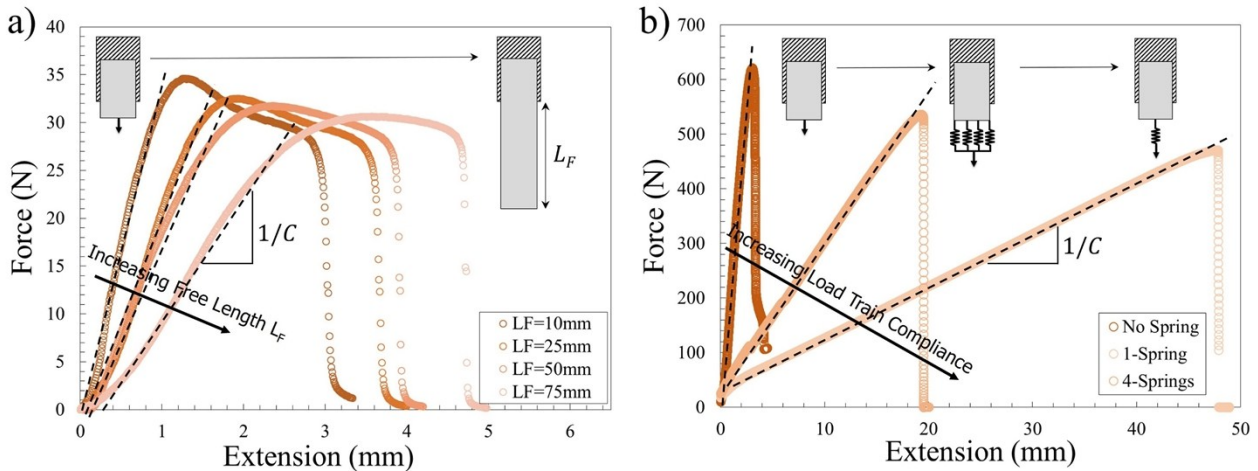


Figure 2. Force versus extension curves of PSA for a) different values of free length L_F and b) different load train compliances

Figure 3 shows the data in Figure 1a, Figure 3a, and Figure 3c in the paper on the log-log scale to demonstrate how many orders of magnitude shear force capacity were tested. Furthermore, as seen in Figure 3, when a log-log scale is used the data appeared to be less scattered compared to the linear scale. Furthermore, there is no distinct difference for the data with different load train compliance shown in Figure 3b, showing that using the data in log-log scale may not illustrate the

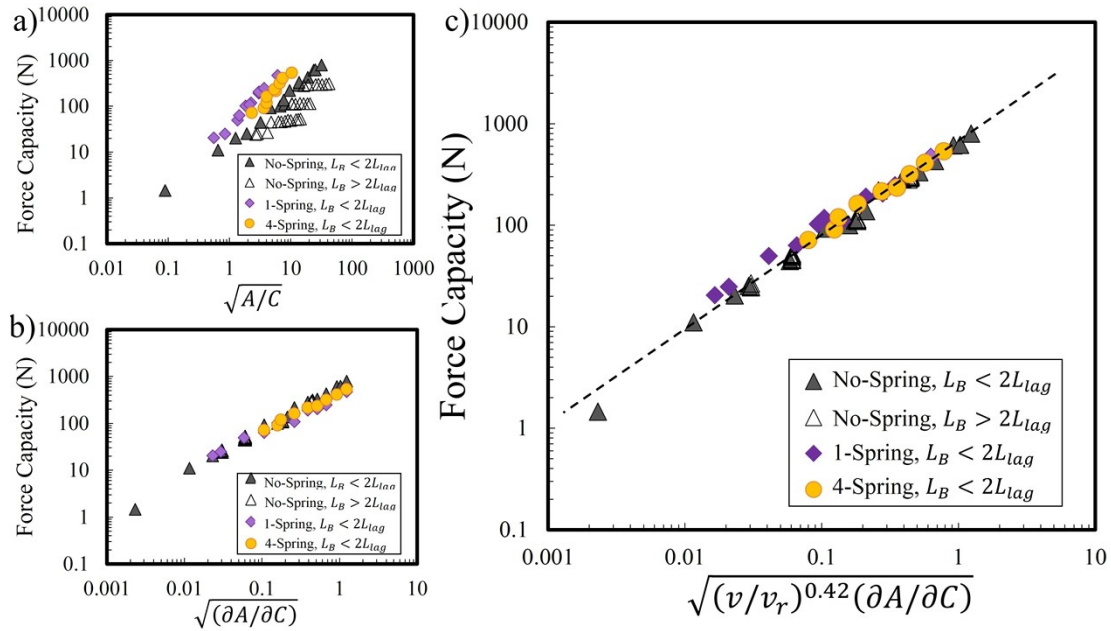


Figure 3. Measured shear force capacity versus: a) experimental scaling parameter b) theoretical scaling parameter without considering rate effect c) theoretical scaling parameter including rate effect in log-log scale.

detailed differences between data points.

Figure 4 exhibits the loading-unloading results for the PSA, showing that the permanent deformation was less than 10% of the total deformation ($\Delta_p/\Delta_T = 7\%$ for 1-layer and 9.5% for 3-layers of PSA tapes) for loading up to 70% of the failure load and believed to be negligible compared to the linear elastic deformation. This also support the linear elastic assumption made in derivation of the scaling parameter based on the fracture mechanics approach.

Furthermore, the rate-dependent response of strain energy release rate was obtained by performing 90 degree peel tests at different peeling velocities to independently calculate the power m in equation (1) in the paper. Figure 5 demonstrates the results for G_c versus peel rate, which is consistent with that of shear test ($m=0.42$ in shear versus $m=0.4$ in 90 degree peel test).

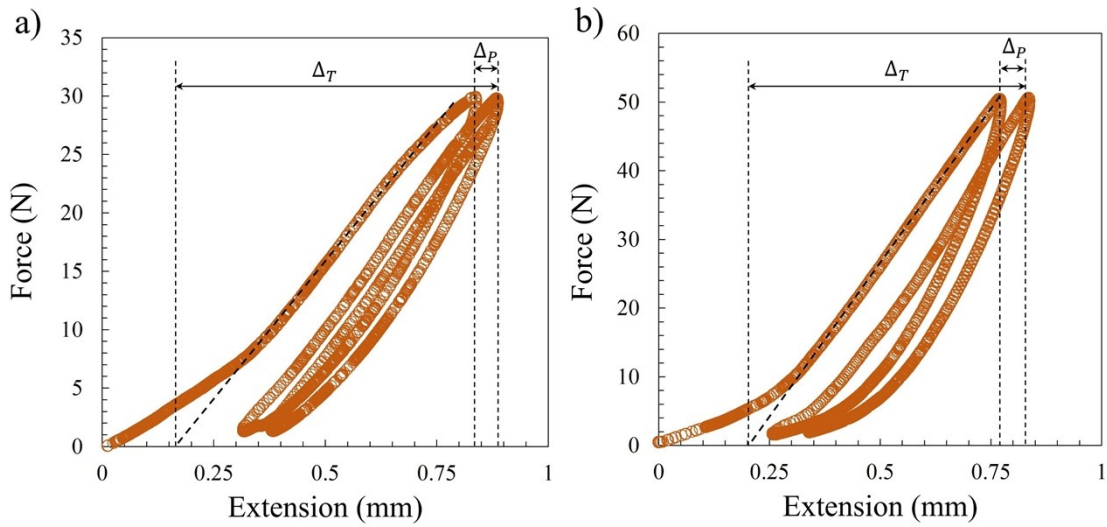


Figure 4. Loading-unloading curve for a) 1-layer of PSA tape b) 3-layers of PSA tape and the corresponding permanent () and total deformations ()

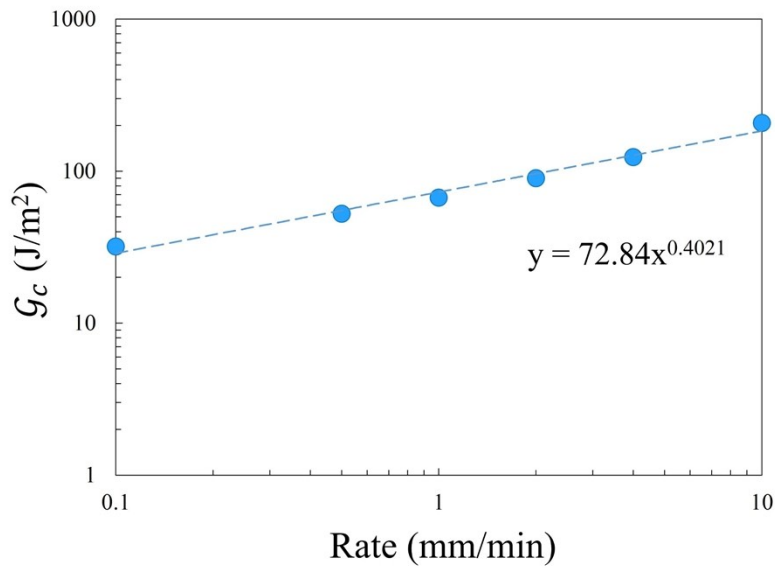


Figure 5. Critical strain energy release rate versus crack propagation velocity of PSA in log-log scale (markers) and the corresponding power-law fit (dash line) obtained from 90 degree peel test. Constant is obtained from the slope and found to be 0.4, consistent with that of shear test.

1. Bartlett, M.D., A.B. Croll, D.R. King, B.M. Paret, D.J. Irschick, and A.J. Crosby, *Looking Beyond Fibrillar Features to Scale Gecko-Like Adhesion*. *Advanced Materials*, 2012. **24**(8): p. 1078-1083.